Investigation of the temperature-dependent failure processes in a PVD Cr-coated ZIRLO nuclear fuel cladding material using real-time X-ray micro-tomography imaging

Guanjie Yuan^{1,2}, Martin Ševeček^{3,4}, Dong (Lilly) Liu^{1,2}

¹Department of Engineering Science, University of Oxford, Oxford, UK

²School of Physics, University of Bristol, UK

³Department of Nuclear Science and Engineering, Massachusetts Institute of Technology,

Cambridge, MA, USA

⁴Faculty of Nuclear Sciences and Physical Engineering, Czech Technical University in Prague,

Prague, Czech Republic

Corresponding author: Dong (Lilly) Liu, dong.liu@eng.ox.ac.uk

1. INTRODUCTION

Zirconium-based alloys (Zircaloys) have been employed as fuel cladding materials in light water reactors (LWRs) for several decades [1]. However, Zircaloys are prone to rapid oxidation in hightemperature steam environments, resulting in significant degradation of mechanical strength and structural integrity. In response to the requirements of accident tolerant fuel (ATF) development [2], Cr has been widely adopted as a protective coating material for Zircaloy claddings [3]. The physical vapour deposition (PVD) method offers distinct advantages and has become one of the most extensively studied techniques for applying Cr coatings to Zircaloy materials [2]. However, most existing studies do not provide real-time 3D characterization of the deformation and failure process of PVD Cr-coated Zircaloy

systems under mechanical loading.

To address this knowledge gap, the present study investigates the real-time mechanical behaviour and failure processes of a PVD Cr-coated Optimized ZIRLO® (Opt. ZIRLO™) cladding. Claddings were sectioned into C-ring specimens and subjected to compressive loading until failure, while real-time synchrotron-based micro X-ray computed tomography (XCT) imaging scanned at room temperature (RT), 345°C, 650°C, and 950°C in an argon atmosphere to capture failure process. Moreover, scanning electron microscopy (SEM) imaging and electron backscatter diffraction (EBSD) mapping were performed on the materials after C-ring loading, to support the findings from real-time XCT imaging.

2. MATERIALS AND EXPERIMENTS

The PVD Cr-coated Opt. ZIRLOTM cladding materials have a wall-thickness (t) of 0.57 ± 0.017 mm, outer radius (r_0) of 4.57 \pm 0.021 mm and inner radius (r_i) of 4.00 \pm 0.016 mm, with one schematic presented in Fig. 1. The thickness of Cr coating is $15.78 \pm 0.42 \,\mu\text{m}$. The in situ high-temperature C-ring

1

compression tests were conducted at Beamline 8.3.2 of the Advanced Light Source at Lawrence Berkeley National Laboratory following the ASTM Standard C1323-16 [4].

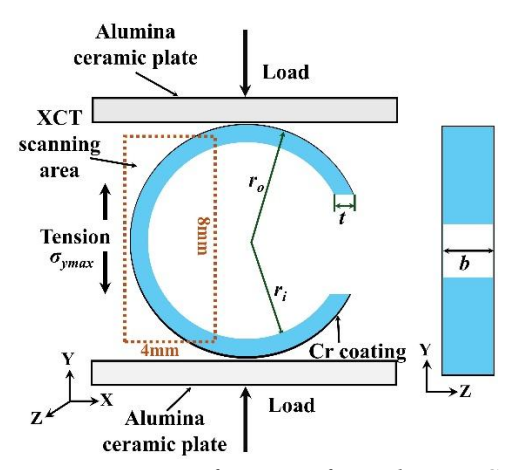


FIG. 1. Schematic of the C-ring compression configuration for real-time XCT testing of cladding materials, including the dimensions of C-ring sample and the coordinate system.

3. RESULTS

For the as-received materials, no obvious pores was found in the Cr coating and at the coating/substrate interface, Fig. 2a. The Cr coating exhibited a predominantly columnar grain morphology. Quantitative analysis revealed an average grain area of $1.1 \pm 0.8 \, \mu m^2$.

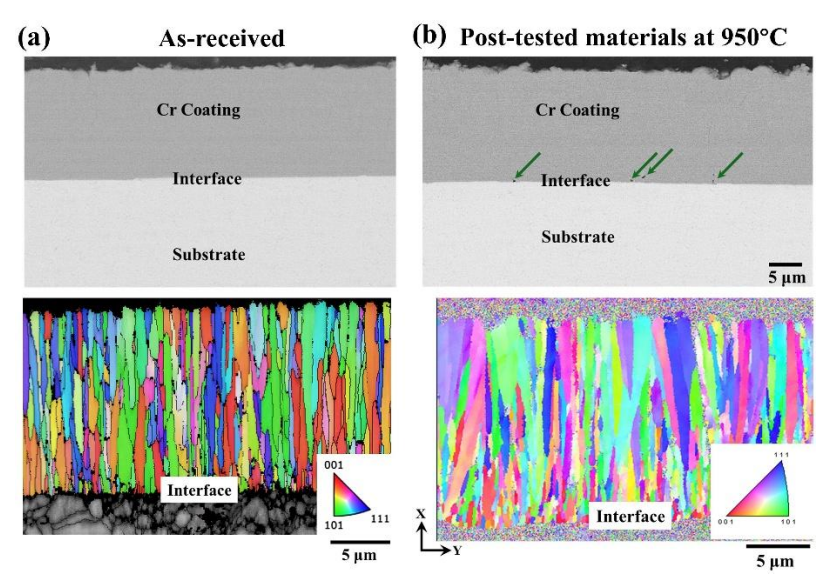


FIG. 2. Polished cross-sections: (a)Microstructure of as-received materials, (b) Microstructure of post-tested materials at 950 °C.

No significant microstructural changes were observed in the materials tested at RT, 345°C, and 650°C. However, specimens tested at 950°C exhibited the formation of pores both at the interface and in the Cr coating adjacent to the interface, Fig. 2b. Moreover, the average area of Cr grains increased to ~5.7 μm², indicating recrystallization of Cr grains occurred during testing at 950°C.

As for the mechanical behaviour, at both RT and 345°C, a linear relationship of load and displacement can be observed at the initial loading stage in the curves, Fig. 3a. At 650°C and 950°C, significant softening of the cladding material was observed, Fig. 3b.

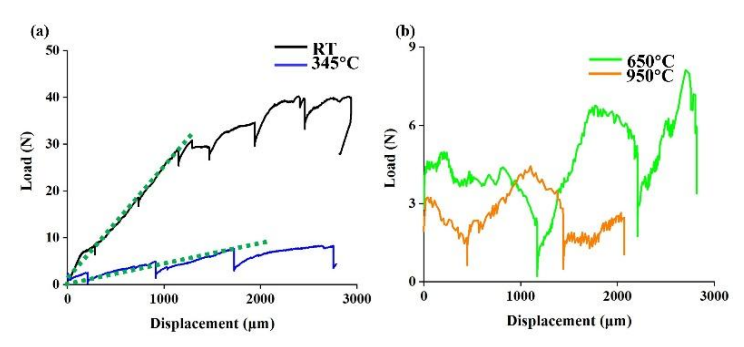


FIG. 3. Mechanical behaviour of the cladding material: (a) at RT and 345°C, (b) at 650°C and 950°C.

For the failure processes, at RT, multiple coating cracks simultaneously formed at ~73% of the peak load (P_U), Fig. 4a. Cracks were arrested at the coating/substrate interface, with cracks travelling almost perpendicular to the hoop direction (88° to 91°). Number of cracks increased with increasing of load. At 345°C, number of coating cracks at P_U were lower compared to RT. Moreover, cracks have a higher angle range against the hoop direction (81° to 96°), Fig. 4b.

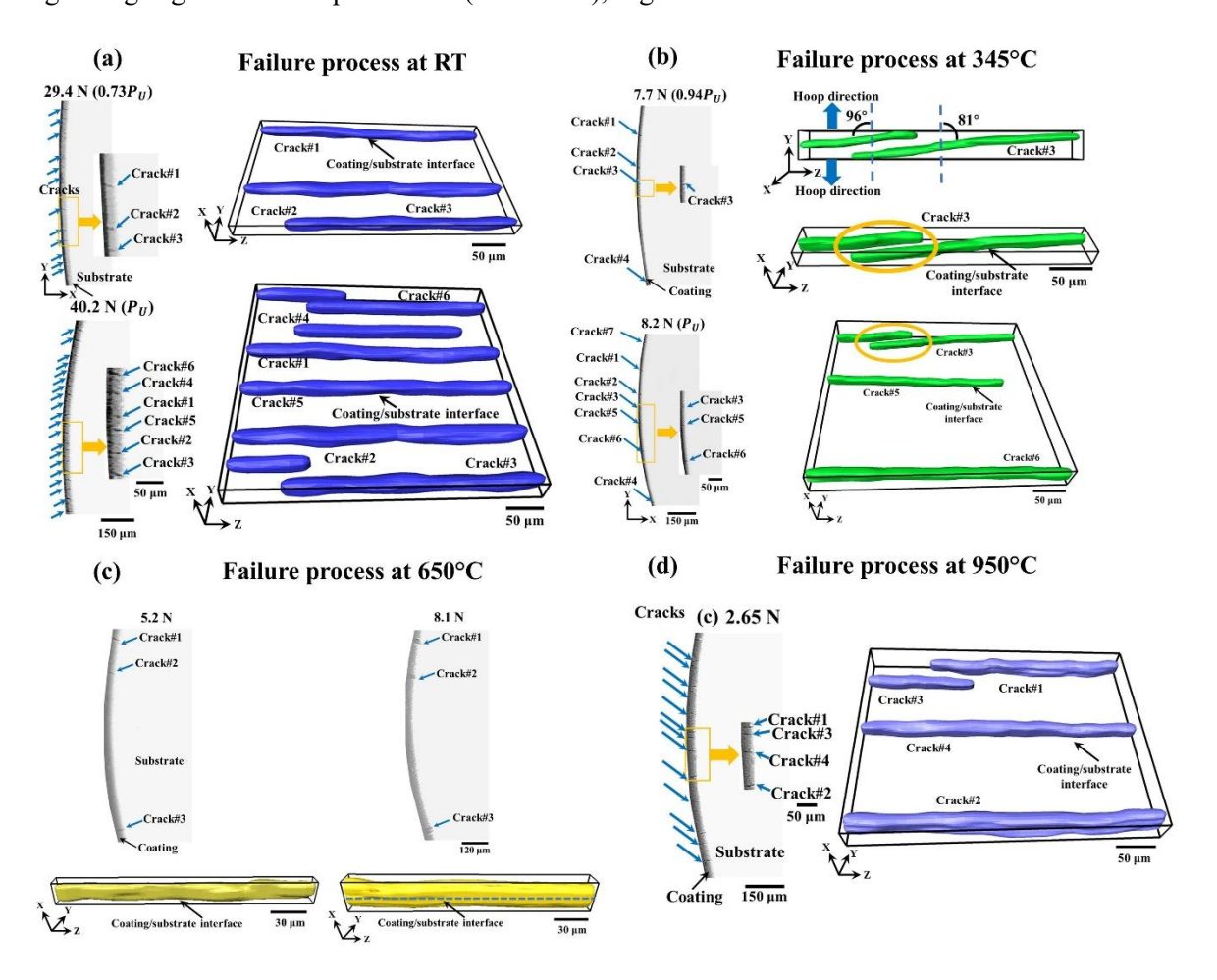


FIG. 4. Real-time failure processes of the cladding material under mechanical loading: (a) at RT, (b)at 345°C, (c) at 650°C and (d) at 950°C.

However, at 650°C, number of cracks did not increasing with increasing of load, but increased in width. Cracks were found travelled into the underlying substrate, Fig. 4c. At 950°C, the number of coating cracks were found again increased with increasing load, and arrested at the coating/substrate interface, Fig. 4d. These indicate the failure of cladding materials underwent brittle to ductile reversion from RT to 650°C, and subsequently ductile-to-brittle reversion from 650°C to 950°C.

4. CONCLUSION

In this study, temperature-dependent failure processes of a PVD Cr-coated Opt. ZIRLO™ cladding material were investigated at elevated temperatures. The observed transition from ductile to brittle fracture mode at extreme temperatures may be attributed to grain growth in the Cr coating during recrystallisation. The enlargement of Cr grains can lead to increased stress concentration within individual grains, thereby promoting brittle fracture behaviour under mechanical loading.

ACKNOWLEDGEMENTS

D.L. acknowledges funding support from UK EPSRC (EP/T000368/1), M.S. acknowledges funding support for the Centre of Advanced Nuclear Technology II (TN02000012) provided by the Technology Agency of the Czech Republic. The authors also acknowledge the use of the X-ray synchrotron microtomography beamline (8.3.2) at the Lawrence Berkeley National Laboratory's Advanced Light Source, which is supported by the Office of Science of the U.S. Department of Energy under contract no. DE-AC02-05CH11231.

REFERENCES

- [1] S. Joung et al., "Post-quench ductility limits of coated ATF with various zirconium-based alloys and coating designs," J. Nucl. Mater., vol. 591, p. 154915, Apr. 2024, doi: 10.1016/j.jnucmat.2024.154915.
- [2] G. Yuan et al., "In situ X-ray computed micro-tomography imaging of failure processes in Cr-coated Zircaloy nuclear fuel cladding materials," Mater. Des., vol. 234, p. 112373, Oct. 2023, doi: 10.1016/j.matdes.2023.112373.
- [3] M. Ševeček et al., "Development of Cr cold spray-coated fuel cladding with enhanced accident tolerance," Nucl. Eng. Technol., vol. 50, no. 2, pp. 229–236, Mar. 2018, doi: 10.1016/j.net.2017.12.011.
- [4] ASTM Standard C1323-26, Standard Test Method for Ultimate Strength of Advanced Ceramics with Diametrally Compressed C-Ring Specimens at Ambient Temperature, ASTM International, West Conshohocken, PA, 2016, https://doi.org/10.1520/C1323-16.2.
- [5] G. Yuan et al., "Investigation of the temperature-dependent failure processes in PVD Cr-coated ZIRLO nuclear fuel cladding using in situ X-ray micro-tomography imaging," Surf. Coat. Technol., vol. 512, p. 132376, Sep. 2025, doi: 10.1016/j.surfcoat.2025.132376.